Hydrol. Earth Syst. Sci. Discuss., 8, 4355–4379, 2011
www.hydrol-earth-syst-sci-discuss.net/8/4355/2011/
doi:10.5194/hessd-8-4355-2011

Hydrology and Earth System Sciences Discussions

Characterizing temporary hydrological regimes at a European scale

M. J. Kirkby[1], **F. Gallart**[2], **T. R. Kjeldsen**[3], **B. J. Irvine**[1], **J. Froebrich**[4], **A. Lo Porto**[5], **and the MIRAGE team**[*]

[1]School of Geography, University of Leeds, Leeds, UK
[2]Surface Hydrology and Erosion Group, Geosciences Department, Institute of Environmental Assessment and Water Research (IDÆA), CSIC, Barcelona, Spain
[3]Centre for Ecology and Hydrology (CEH), Wallingford, UK
[4]Centre for Water and Climate (CWK), Integrated Water Resources Management, Alterra, Wageningen, The Netherlands
[5]Water Research Institute IRSA-CNR, Bari, Italy
[*]MIRAGE project (Mediterranean Intermittent River ManAGEment): 7th EU Framework Programme, coordinated by J. Froebrich, Centre for Water and Climate (CWK), Integrated Water Resources Management, Alterra, Wageningen, The Netherlands

Received: 25 March 2011 – Accepted: 12 April 2011 – Published: 29 April 2011

Correspondence to: M. J. Kirkby (m.j.kirkby@leeds.ac.uk)

Published by Copernicus Publications on behalf of the European Geosciences Union.

Abstract

Monthly duration curves have been constructed from climate data across Europe to help address the relative frequency of ecologically critical low flow stages in temporary rivers, when flow persists only in disconnected pools in the river bed. The hydrological model is based on a partitioning of precipitation to estimate water available for evapotranspiration and plant growth and for residual runoff. The duration curve for monthly flows has then been analysed to give an estimate of bankfull flow based on recurrence interval. The corresponding frequency for pools is then based on the ratio of bank full discharge to pool flow, arguing from observed ratios of cross-sectional areas at flood and low flows to estimate pool flow as 0.1% of bankfull flow, and so estimate the frequency of the pool conditions that constrain survival of river-dwelling arthropods and fish. The methodology has been applied across Europe at 15 km resolution, and can equally be applied under future climatic scenarios.

1 Introduction

Many of our hopes (Sivapalan et al., 2003) of providing a basis for making predictions in ungauged drainage basins have stalled on the unexplained dissimilarities of apparently similar basins. Here we focus on the impact of climatic inputs on the hydrologic responses of catchments, paying particular attention to their low flow characteristics and how these are controlled by the seasonality of climate, the response of vegetation cover and the interactions with evapotranspiration and runoff throughout the year. It is hoped that differences in monthly duration curves, analysed here, can provide one tool for looking at and classifying the characteristic signatures of climate and the contrasting hydrological regimes that are driven by climatic differences. By looking for major differences across a wide range of catchments, we deliberately focus on the climatic signal that distinguishes between, for example, snow-dominated, humid and semi-arid

HESSD

8, 4355–4379, 2011

regimes. Although unusual in being applied to monthly flows, the methods of duration flow analysis follow those recommended by Vogel and Fennessey (1994), representing the duration curves as log normal/probability plots as recommended by Searcy (1959).

We take a very simple hydrological model, focussing on monthly time steps with a superimposed distribution of daily storm rainfalls, to generate monthly flow duration curves from climatic data. At this time resolution, routing and quickflow responses play a minor part except in very large catchments (>10^5 km^2) so that the appropriate hydrological model is one dominated by recession behaviour. Our intention has been to parameterise this model to reflect the indirect effects of climatic differences, notably through vegetation.

The work reported here focuses on low flow characteristics in semi-arid catchments, particularly when flow is spatially discontinuous and/or confined to disconnected pools. We are looking for regional patterns that will help define areas with different types of hydrological response in order to guide the management of non-permanent water bodies, and provide criteria of good ecological status where surface flow is occasionally to frequently absent. We are therefore attempting to model broad regional patterns in the frequency of these 'pool' conditions, and examine how this frequency varies through the year. At present the approach is exploratory, proposing principles to apply rather than providing definitive conclusions.

The meteorological data is mainly from CRU (New et al., 2002; Mitchell et al., 2003) interpolated average data for a spatial grid of 10 min of arc (c 15 km), so that simulations are generated for source areas of c 200 km^2. These data are used to generate 50-year synthetic climate records without trends. Potential evapotranspiration (ET) is not included in these data, and has been estimated using the Hargreaves (Hargreaves and Samani, 1982) method, based on incoming solar radiation and temperature. The core of the model is designed to partition precipitation into the components of Infiltration excess and saturation excess overland flow, subsurface flow and actual ET. Actual and Potential ET are then used to interactively estimate uncultivated plant cover, vegetation biomass, soil organic matter biomass and runoff thresholds. The model is spun up for

HESSD
8, 4355–4379, 2011

five years to stabilise the hydrology and then run for the 50-year period to generate a synthetic monthly flow exceedance curve.

Although there are many local factors that influence hydrological response, including the presence of aquifers, variations in soil properties, imposed land use and water abstractions or return of treated wastewater, these have not been incorporated into the model presented here, allowing broad patterns of difference to emerge that are related to climatic differences and their impact on the hydrological regimes. The model has been developed in the context of the EU MIRAGE project, on water management in southern Europe, so that the examples used largely reflect concern with ecological status of temporary rivers, which is intimately linked to the presence or absence of disconnected or zero surface flow during the summer period.

2 Model structure

2.1 Construction of synthetic climate time series

The CRU European and Global 10-min databases (New et al., 2002; Mitchell et al., 2003) contain averages for monthly total precipitation and its standard deviation, and number of rain days per month. They also contain data for temperatures and mean values of vapour pressure or relative humidity. The European data base also contains year by year monthly values for 1901–2000, and these data are sufficient to estimate monthly potential ET, using the Hargreaves method (Hargreaves and Samani, 1982), for each month, and consequently mean and standard deviation for each month. This method estimates top of atmosphere radiation from latitude, and air temperature to modify this to make some correction for cloudiness. Additional ERA-40 data have been added (BADC) for the coefficient of variation of rain on rain-days, averaged for the same spatial grid.

These data have then been used to define distributions, and a 50-year time series has been generated by drawing independent samples from these distributions. Monthly

Discussion Paper | Discussion Paper | Discussion Paper | Discussion Paper |

HESSD

8, 4355–4379, 2011

Characterizing temporary hydrological regimes at a European scale

M. J. Kirkby et al.

rainfall has been drawn from a gamma distribution defined by the monthly mean and standard deviation. The number of rain days has been adjusted from the mean value by the square root of the ratio of monthly rainfall to average monthly rainfall. In this way, months with higher than average rainfall are assumed to partition this between increases in number of rain days and mean rain per rain day. The coefficient of variation for rain-days has been kept constant at the average monthly value. Monthly potential ET has been drawn independently at random from a normal distribution. Figure 1 shows one visualisation for an example series, near Foggia, Apulia. The web of lines shows the relationship between precipitation and temperature for every month of the 50 year period. The other lines show the monthly averages for precipitation, and the mean monthly potential ET, also plotted against mean monthly temperature. It can be seen that in this Mediterranean climate, rainfall generally exceeds potential ET during the winter period and is less that Pot ET during the summer, although with substantial year to year variations. This pattern realistically reflects long term observed data.

2.2 Hydrological model

The hydrological model is designed to partition precipitation into its components (Fig. 2), and is a simplified version of that used in the PESERA regional soil erosion model (Kirkby et al., 2008). The key elements of the model estimate actual ET and the elements of runoff in relation to precipitation and soil moisture.

For actual ET, some water is taken directly from rainfall for rain days, limited by daily evaporative demand in relation to the distribution of available daily rain amounts. If the evaporative demand has not been satisfied from this near-surface water, vapour is additionally drawn from the subsurface saturated zone, balancing changes in water deficit against percolating residual rainfall, drainage and evaporative demand from vegetated and bare fractions of the surface, as a function of deficit and rooting depth. This allows ET to follow potential ET in wet conditions, and to draw down soil moisture in dry conditions, while never exceeding either potential I ET or precipitation over the water year.

HESSD
8, 4355–4379, 2011

The runoff components represent infiltration excess and saturation excess processes. Infiltration excess overland flow is estimated by summing the daily rainfalls in excess of a runoff threshold. This methodology is inherited from the PESERA model, where it has provided the basis for estimating soil erosion based on the month by month distribution of these runoff amounts. Although there are limitations in using daily rainfalls, this simplification has been used as a compromise between our understanding of the processes and the availability of regional data at finer time resolutions. After allowing for losses or gains from snow fall or snowmelt, from infiltration excess overland flow and from near-surface evaporation, the residual net rainfall percolates to a saturated sub-surface zone. The saturation deficit is updated for fractions (normally one fifth) of a month, balancing percolation against losses due to drainage (as lateral subsurface flow) and ET from the saturated zone. Actual subsurface ET is estimated from the available water and evaporative demand, using a modification of the Budyko approach (Pike, 1964; Arora, 2002). Subsurface drainage is estimated using the most basic version of TOPmodel (Beven and Kirkby, 1979), in which lateral flow decreases exponentially with increases in saturation deficit. Where saturation deficit falls to zero, a third component of runoff, as saturation excess overland flow, is also estimated.

Input is taken monthly from the synthetic time series. First precipitation is partitioned into rain and snow on the basis of temperature. The snowpack gains from snowfall, and loses snowmelt, estimated from a day-degree model to give an effective rainfall. Infiltration excess overland flow is estimated from a runoff threshold that varies in response to vegetation cover and soil organic matter. The distribution of daily rainfalls for each month is fitted to a Gamma distribution and the overland flow estimated by summing over the frequency distribution of rainfalls in excess of the threshold. The distribution of daily rainfalls is also used to estimate the amount of water that is available for near-surface ET.

The residual rainfall percolates into the soil, and the month is subdivided to update the saturation deficit in stages to maintain computational stability, allowing for subsurface flow and saturation excess overland flow when appropriate. There is also a

HESSD
8, 4355–4379, 2011

loss by further ET from the saturated zone, calculated separately for vegetated and bare areas. Combining these components provides an estimate for total actual ET, plant water use (pro-rated to cover) and the several components of runoff by overland and subsurface pathways.

Plant water use is then used to estimate vegetation and soil organic matter biomass. Although a transient model might be desirable, it was recognised that times for equilibration, particularly for organic matter in potentially saturated environments, might be excessive, so that biomass was calculated for equilibrium conditions, updated annually to allow for minor changes in response to climate variability. Finally cover and biomass were used to update the runoff threshold, providing a dynamic link between overland flow runoff and vegetation in response to the prevailing climate.

2.3 Exceedance curves and other indicator tools

The model is based on runoff generation from source areas, and assumes that all runoff pathways contribute to stream flow downstream. Exceedance curves were generated from the combined total runoff contributions for each month, providing a basis that, in our experience, could be most reliably compared with observed data. These were sorted and presented as a plot of log(monthly discharge) against probability of exceedance, plotted on a probability scale or z-score, so that a log-normal distribution of discharges appears as a straight line. Since, we wish to analyse the frequency of low flow conditions, we have preferred to use the complete synthetic record, rather that partition it from the ouset on the basis of dry periods, as has been proposed by Viola et al. (2011). Examples are shown in Fig. 4.

Five catchments have been chosen across a range of environments to examine the response of the exceedance curves to climate. Table 1 summarizes their characteristics, showing their position, precipitation and estimated potential ET. It can be seen that the catchments range from semi arid, with precipitation less than half potential ET, to humid with precipitation exceeding potential ET, and with a range of seasonality.

HESSD
8, 4355–4379, 2011

These test catchments have been used to test whether the hydrological model is able to distinguish broad differences in duration curve characteristics without specific optimisation of parameters for each site.

The model is driven by three significantly changeable parameters. The first of these is the TOPmodel "m" parameters, which describes the rate at which subsurface drainage decreases as saturation deficit increases, and has the dimensions of depth (mm of water). High values of m provide some subsurface flow even at high deficits, and give long-tailed recession curves. Whereas low values of m give flashy response, with negligible flow at high saturation deficit. The value of m scales the deficits (and implicitly depths) to which water will drain.

The second control parameter is the rooting depth under vegetation, R, which is also expressed as a water deficit. Vegetation is able to extract transpiration water readily under conditions when the deficit is less than the rooting depth, and progressively less as the deficit increases. Bare soil evaporation is also allowed, but with a small (5 mm) scale depth, and total transpiration loss combines bare soil and plant transpiration according to the prevailing crown and root cover.

The third parameter is the subsurface runoff at saturation, j_*. This is important for partitioning between subsurface and saturation excess overland flow, and is increasingly important as the simulation time step is reduced, but has little impact on total runoff for the monthly time steps used here. Other parameters control the rate of conversion of plant transpiration to biomass, respiration, leaf etc. fall and decomposition, and these have been taken from values used in the PESERA model, and taken from the literature without further adjustment.

For suitable climatic areas, the model shows three main response zones to the two primary parameters. First a zone in which rooting depth is much less than TOPmodel m. Here the response is dominated by subsurface and saturation excess overland flow, with little sensitivity to the vegetation. In humid areas, the soil is frequently close to saturation, and plant growth is unrestricted by water. In more arid areas, few of these shallow-rotted plants are able to survive. In a second zone, where rooting depth

HESSD
8, 4355–4379, 2011

is substantially greater than TOPmodel m, the hydrology is dominated by root extraction, with minimal lateral subsurface drainage. Under humid conditions, most runoff occurs as saturation excess overland flow, while in semi-arid conditions deep-rooted plants exploit percolating storm rainfall. However, the response of the catchments investigated all lay between these extremes, in a zone where both subsurface flow and plant transpiration play a part. Where the climate is seasonal, then dry seasons are typically dominated by root extraction, and wet seasons by increased subsurface flow.

For the five test catchments, the goodness of fit of the modelled duration curve was estimated from the average root mean square (RMS) difference between observed and estimated log(discharge) across the range of non-zero values. To minimise inconsistencies, the same climate realisation was used for each parameter pair, and each different realisation produces a slightly different error map. Figure 3a shows an example for the Hozgarganta catchment, over the ranges $m = 2–52$ mm; $R = 10–210$ mm. It can be seen that there is a weakly defined optimum at $m = 6$ mm; $R = 54$ mm, within a trough-shaped region in which m and R increase together, maintaining moderately low values of the RMS error. Similar mappings can be made for the other catchments, and Fig. 4 shows the optimum values of m and R for each. Comparing these values, it can be seen that higher values of m are generally associated with higher values of R. It is therefore suggested that a single global parameter set might encapsulate much of the significant climatic difference across all sites.

To estimate the best global values, individual error maps for each site (similar to Fig. 3a) have been normalised to (RMS value–Minimum value)/(Maximum value–Minimum Value), so that each error map is linearly transformed to the range [0,1]. Figure 3b is then obtained as the average of the five normalised error maps, and itself shows a minimum, with an average of 13.4% deviation from the individual optima. This minimum sets the global parameter values at $m = 6$ mm; $R = 50$ mm. An alternative criterion is, for each parameter set, to map the largest of the normalised errors for the test catchments; and select the least maximum (27%), a minimax solution that gives parameter values of $m = 6$ mm; $R = 60$ mm. The former values have been used, giving

HESSD
8, 4355–4379, 2011

a minimax normalised error of 32%.

For each of the five test catchments, Fig. 4 shows the exceedance curves plotted from the observed data, and with simulated curves generated with the local best fit parameter set and the global set. It can be seen that differences between the three curves for each site are much smaller than the differences between the five sites, and this encourages us to use the global parameter values to simulate regional patterns of natural variation in the exceedance curves. It is recognised that many factors are not taken into account in this analysis, including the impact of non-natural vegetation, abstraction of water for irrigation, domestic use and industry, return of urban waste water and exchange with aquifers, particularly karst aquifers.

3 Analysis of low flow conditions from exceedance curves

To interpret low flow conditions for streams in different climates, we have used the concept of bank full discharge to provide a generalised measure of channel dimensions, and have used the well known, although not necessarily totally reliable, method of associating bank full discharge with a frequency of occurrence. An exceedance with a z-score of −2.5, corresponding to a probability of 0.62%, or 3.7 months in 50 years. Here we are using a rarer event than that normally used to define bank full flows (1–5–10 year Recurrence interval) to compensate for the use of monthly total flows (Leopold, 1994; Pickup and Warner, 1975), but which is still within the range of flows observed and modelled with a 50 year synthetic climate series. This discharge is used to indicate the cross sectional area of the bank full channel. Since at-a-station discharge is approximately proportional to Cross sectional area to a power, typically 0.6 (Leopold and Maddock, 1953), then reductions in discharge correspond to reductions in wetted cross-sectional area. Table 2 shows observed ratios between bank full discharges and discharges at which disconnected pools are present for a set of catchments in southern Europe studied in the MIRAGE project. The geometric mean of the listed flood:pool discharge ratios is 1100, and the median is 950. From these data it is proposed to use a discharge ratio of 1000 as an indicator of pool conditions, and this should correspond to a cross-sectional ratio of $1000^{1/0.6}$, i.e. 10^5. An intermediate "riffle" stage has also been used for illustrative purposes, corresponding to a discharge ration of $\sqrt{}(1000)$, or a cross-sectional area ratio of 300. At this level continuous flow is anticipated, but without drowning out riffles and similar features.

Figures 5 and 6 show the regional aridity and the predicted frequency of pools under the current climate. In Fig. 5, aridity is indicated by the average number of months per year with precipitation less than 60% of potential evapotranspiration. There is a clear north south gradient with many Mediterranean areas having more than 4.5 dry months in the summer. In Fig. 6, the model has been applied to show the frequency of "pool" conditions throughout the year. It can be seen that the forecast pattern, although identifying the same north south differences, has a much sharper concentration towards the south.

Figure 7 shows the corresponding distribution with a uniform 2 °C rise in temperature. It can be seen that the differences are small, but generally in the direction of a small reduction in the frequency of pool conditions. The temperature rise increases potential ET, and this has some effect on natural vegetation biomass, which increase where there is adequate rainfall. There is a consequent reduction in runoff, which decreases both flood and low flows. It is therefore argued that the short term impact of a step rise in temperature may be some increase in low flow (pool) frequency but that, after a while, bankfull channel dimensions will decrease, largely counteracting the initial change.

Although there is substantial variability, there is a general relationship between the mean value of forecast pool frequency and the number of dry months per year, and this relationship is little changed by a 2 °C temperature rise. Figure 8 shows that this average behaviour is non-linear with a more rapid increase in pool frequency above about 4 dry months per year, which is consistent with the strong concentration apparent in Figs. 6 and 7 towards southern Europe and the Mediterranean.

HESSD
8, 4355–4379, 2011

4 Conclusions

The model presented shows some potential for estimating the hydrological impact of climate in time and space, containing a number of feedback paths, mainly through vegetation, that influence the partition of precipitation between evapotranspiration and runoff. The use of the monthly duration curve provides a rather stable indicator of overall behaviour, particularly at low flows, and has been shown to allow the use of global parameter sets, in the first instance, rather than requiring individual optimisation for each site.

Appendix A

Model equations

Monthly infiltration excess overland flow is summed over distribution of daily rainfalls for which rainfall r is greater than the runoff threshold h_C.

$$q_{OF} = N \int_{h_c}^{\infty} (r - h_c) \cdot \frac{r^{\alpha-1}}{\beta\,\Gamma(\alpha)} \exp\left(-\frac{r}{\beta}\right) dr \tag{A1}$$

where N is the number of rain days,
h_C is the current runoff threshold,
r is the daily effective rainfall,
α is the Gamma parameter = (Mean daily rainfall)/(standard deviation of rain on rain days),
B is the ratio (mean rain per rain day)/α.
And Γ represents the Gamma function.
Monthly near-surface evapotranspiration is similarly summed for days when effective rainfall is greater than the potential ET demand.

Discussion Paper | Discussion Paper | Discussion Paper | Discussion Paper |

HESSD

8, 4355–4379, 2011

Characterizing temporary hydrological regimes at a European scale

M. J. Kirkby et al.

$$\mathrm{aet_S} = N\left[\int_0^e r\cdot\frac{r^{\alpha-1}}{\beta\,\Gamma(\alpha)}\exp\left(-\frac{r}{\beta}\right)dr + e\int_e^\infty \frac{r^{\alpha-1}}{\beta\,\Gamma(\alpha)}\exp\left(-\frac{r}{\beta}\right)dr\right] \quad \text{(A2)}$$

where e is the lesser of daily evaporative demand or the runoff threshold, h_c.
The ET from the saturated zone is estimated form the relationship

$$\mathrm{aet_d} = 1/\sqrt{\left(1/A^2 + 1/E^2\right)} \quad \text{(A3)}$$

where the available water,

$$A = R\exp(-D/R), \quad \text{(A4)}$$

In which R is the rooting depth and D is the saturation deficit (or zero if it is negative). And E is the (residual) potential ET demand.
This subsurface ET component is calculated separately for vegetated and bare fractions of the surface, and combined to provide the total actual ET, and the plant water uptake.
Subsurface deficit is updated by solving the TOPmodel equations:

$$\begin{aligned}\frac{dj}{dt} &= \frac{j\cdot(i-j)}{m}\\ j &= j_*\exp(-D/m)\end{aligned} \quad \text{(A5)}$$

where j is the subsurface runoff rate, i is the net rate of percolation to the saturated zone = Net Rainfall–Overland flow–Actual ET and m is the TOPmodel soil depth parameter. Equations (3)–(5) are normally solved by subdividing the month into five, progressively updating each component to its monthly total. Cover is modified monthly, always converging towards the value $\sqrt{\frac{\text{Plant water uptake}}{\text{Potential ET}}}$, but with 50% inertia, and Root cover, which is taken to be more complete than surface cover, is estimated as $\sqrt{(\text{Cover})}$. Equilibrium Plant and Soil organic matter biomass are estimated annually, from the equations:
Gross primary productivity = respiration + Leaf Fall

Leaf Fall = SOM decomposition
where GPP ~ Plant Water Uptake,

$$\text{Respiration} \sim \exp\left(\frac{T - 10}{8}\right) \quad \text{(A6)}$$

In which T is temperature in °C,

$$\text{Leaf fall} \sim \frac{V}{\log(V + 1.4)} \quad \text{(A7)}$$

In which Vegetation biomass, V, is in kg m^{-2}, and

$$\text{Annual decomposition} = \{\exp[0.05 \exp(0.12\,T)] - 1\}\,H \quad \text{(A8)}$$

In which H is the SOM biomass.
Finally the runoff threshold h_c, is estimated as

$$h_c = 10 + 40\,C + 50\left[1 - \exp\left(-H/10\right)\right]C, \quad \text{(A9)}$$

where C is the fractional crown cover.

Acknowledgements. The research described here was supported by the EU 7th Research Framework Programme in the MIRAGE project (Mediterranean Intermittent River ManAGEment), No 211732.

References

Arora, V. K.: The use of thearidity index to assess climate change effect on annual runoff, J. Hydrol., 265, 164–177, 2002.
BADC: http://badc.nerc.ac.uk/view/badc.nerc.ac.uk__ATOM__dataent_ECMWF-E40, last access: March, 2011.
Beven, K. J. and Kirkby, M. J.: Towards a simple, physically based, variable contributing area model of catchment hydrology, Int. Ass. Hydrol. Sci. Bull., 24, 43–69, 1979.

HESSD
8, 4355–4379, 2011

Hargreaves, G. H. and Samani, Z. A.: Estimating potential evapotranspiration, ASCE J. Irrig. Drain. Div., 108, 225–230, 1982.
Kirkby, M. J., Irvine, B. J., Jones, R. J. A., Govers, G., and the PESERA team: The PESERA coarse scale erosion model for Europe: I – Model rationale and implementation, Eur. J. Soil Sci., 59(6), 1293–1306, 2008.
Leopold, L. B.: A view of the river, Harvard University Press, Cambridge, 1994.
Leopold, L. B. and Maddock, T.: The Hydraulic Geometry of Stream Channels and Some Physiographic Implications, USGS professional Paper 252, 56 pp., 1953.
Mitchell, T. D., Carter, T. R., Jones, P. D., Hulme, M., and New, M.: A comprehensive set of climate scenarios for Europe and the Globe, Tyndall centre Working paper 55, 2003.
New, M., Lister, D., Hulme, M., and Makin, I.: A high resolution data set of surface climate over global land areas, Clim. Res., 21, 1–25, 2002.
Pickup, G. and Warner, R. F.: Effects of hydrologic regime on magnitude and frequency of dominant discharge, J. Hydrol., 29, 51–75, 1976.
Pike, J. G.: The estimation of annual runoff from metorological data in a tropical climate, J. Hydrol., 2, 116–123, 1964.
Searcy, J. K.: Flow Duration curves, USGS Water Supply paper 1542-A, 1959.
Sivapalan, M., Takeuchi, K., Franks, S. W., Gupta, V. K., Karambiri, H., Lakshmi, V., Liang, X., McDonnell, J. J., Mendiondo, E. M., O'Connell, P. E., Oki, T., Pomeroy, J. W., Schertzer, D., Uhlenbrook, S., and Zehe, E.: IAHS decade on predictions in Ungauged Basins (PUB), 2003–2012: Shaping an exciting future for the hydrological sciences, Hydrolog. Sci. J., 48, 857–880, 2003.
Viola, F., Noto, L. V., Cannarozzo, M., and La Loggia, G.: Regional flow duration curves for ungauged sites in Sicily, Hydrol. Earth Syst. Sci., 15, 323–331, doi:10.5194/hess-15-323-2011, 2011.
Vogel, R. M. and Fennessey, N. M.: Flow Duration Curves, I: New interpretations and confidence limits, J. Water Res. Pl.-ASCE, 120, 485–504, 1994.

HESSD
8, 4355–4379, 2011

Characterizing temporary hydrological regimes at a European scale

M. J. Kirkby et al.

Table 1. Summary characteristics of catchments studied.

Name	Latitude (° N)	Longitude (° E)	Precipitation (mm)	Potential evapo-transpiration
Hozgarganta, Spain	36.4	−5.4	699	1053
Cal Rodo, Spain	42.2	1.9	989	776
Algali, Portugal	39.1	−7.2	640	1170
Kendal, UK	54.4	−2.7	2064	577
Celone San Vincenzo, Italy	41.3	15.5	465	991

HESSD

8, 4355–4379, 2011

Characterizing temporary hydrological regimes at a European scale

M. J. Kirkby et al.

Table 2. Ratios of flood to pool discharges reported for some MIRAGE catchments.

Catchment	Flood: Pool discharge ratio
Salsola – Casanova, Italy	400
Salsola – Ponte Foggia, Italy	400
Celone – S. Vincenzo, Italy	1500
Celone – Ponte Foggia, S. Severo, Italy	2000
Vrontanno, Greece	20 000
Tordera, Spain	200

HESSD
8, 4355–4379, 2011

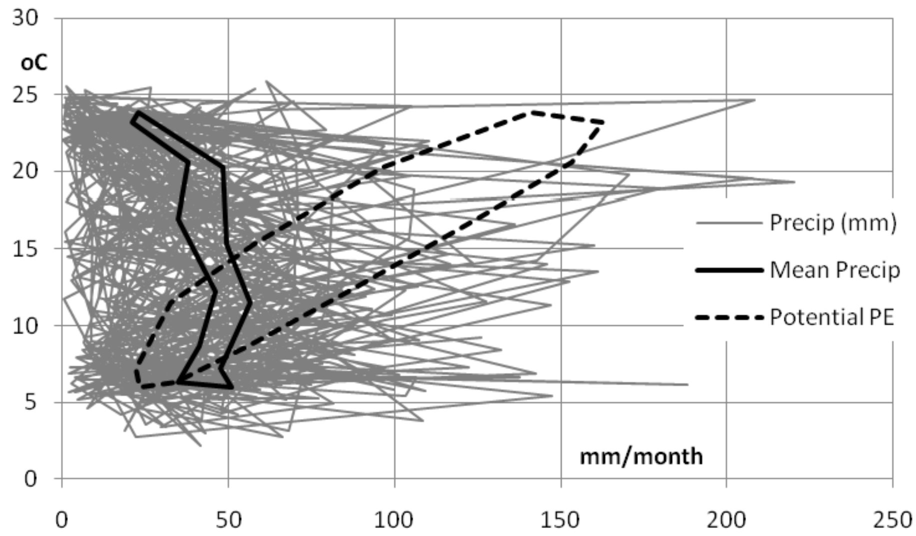

Fig. 1. Example of 50-year synthetic climate realisation for the Celone catchment, near Foggia.

HESSD
8, 4355–4379, 2011

Characterizing temporary hydrological regimes at a European scale

M. J. Kirkby et al.

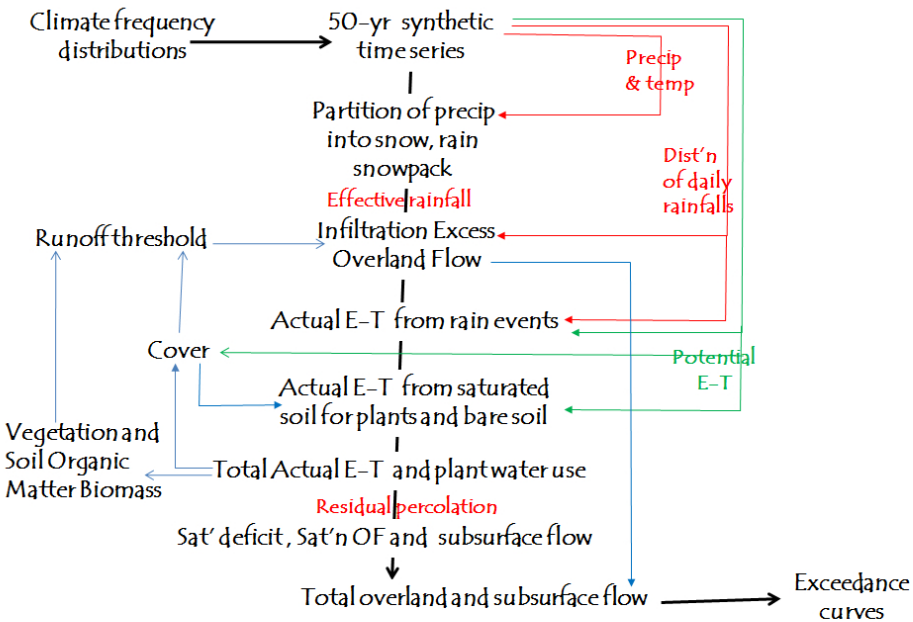

Fig. 2. Schematic for hydrological model.

HESSD
8, 4355–4379, 2011

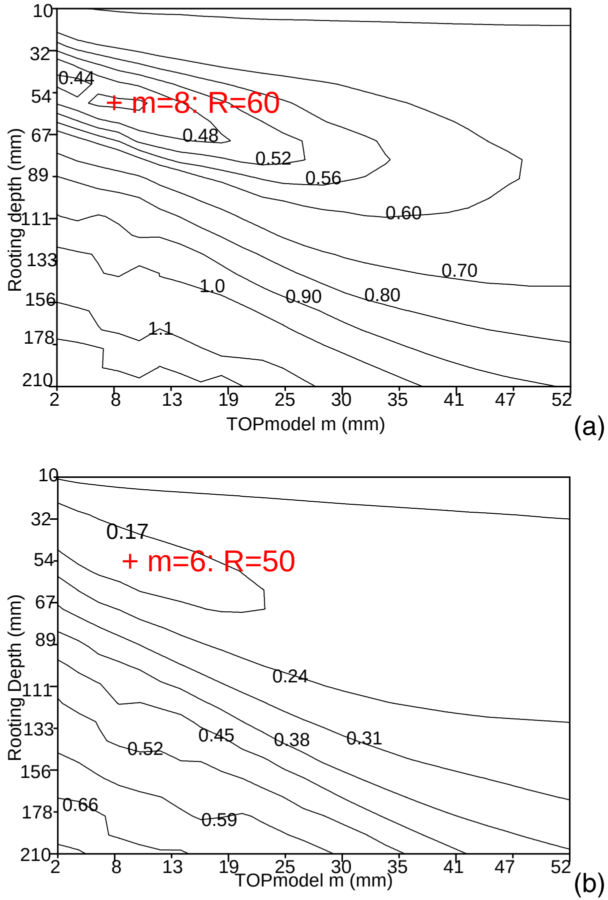

Fig. 3. **(a)** RMS mean difference between observed and simulated exceedance curves for R. Hozgarganta, S. Spain. Δ shows catchment optimum. **(b)** Average normalised departure averaged across five test catchments from their individual minimum RMS error. Δ shows global optimum.

HESSD

8, 4355–4379, 2011

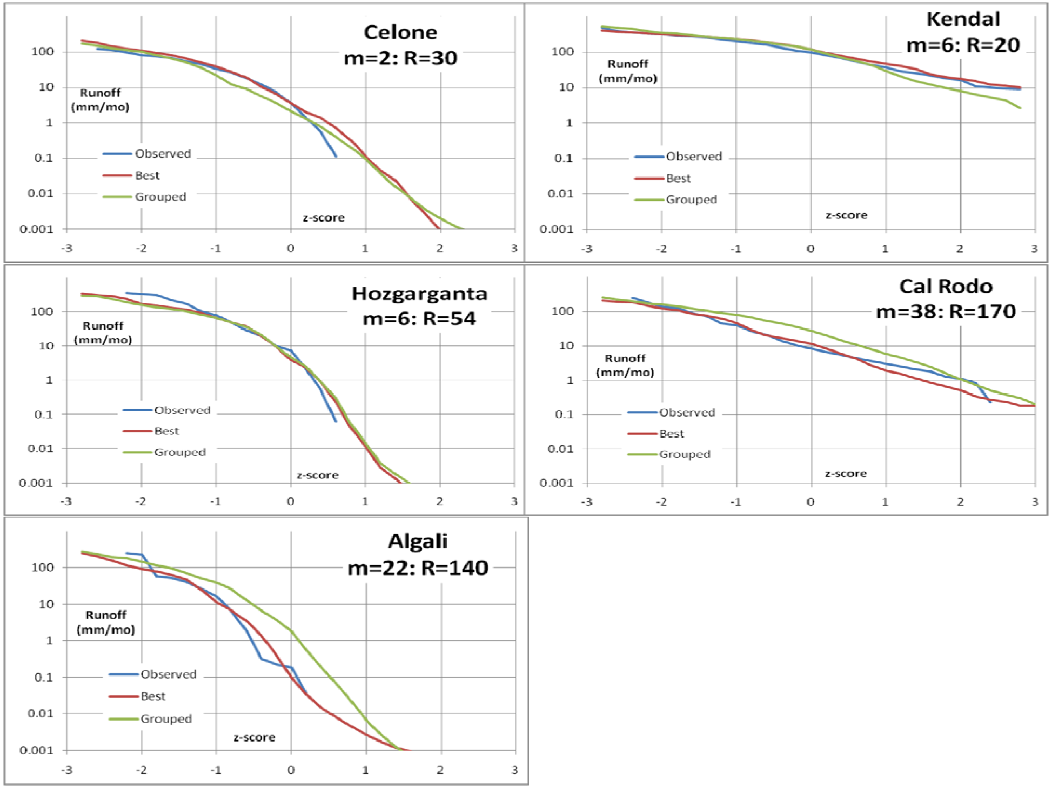

Fig. 4. Exceedance curves for the five test catchments. Each graph shows the observed data, the individual best fit model and the global best fit model.

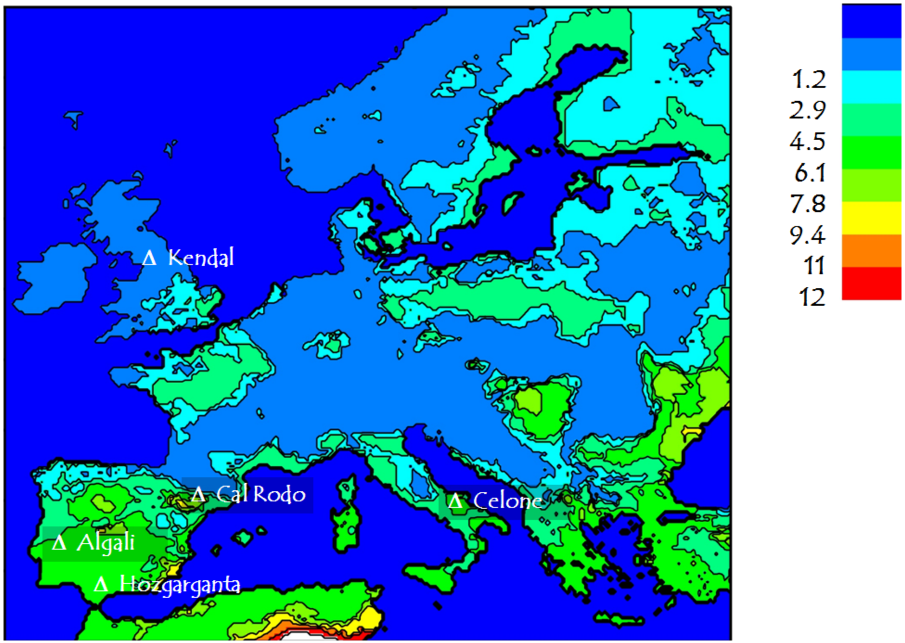

Fig. 5. Average number of months with Precipitation < 0.6 Potential ET. Figure also shows location of test catchments.

HESSD

8, 4355–4379, 2011

Characterizing temporary hydrological regimes at a European scale

M. J. Kirkby et al.

Title Page
Abstract Introduction
Conclusions References
Tables Figures
◂ ▸
Back Close
Full Screen / Esc
Printer-friendly Version
Interactive Discussion

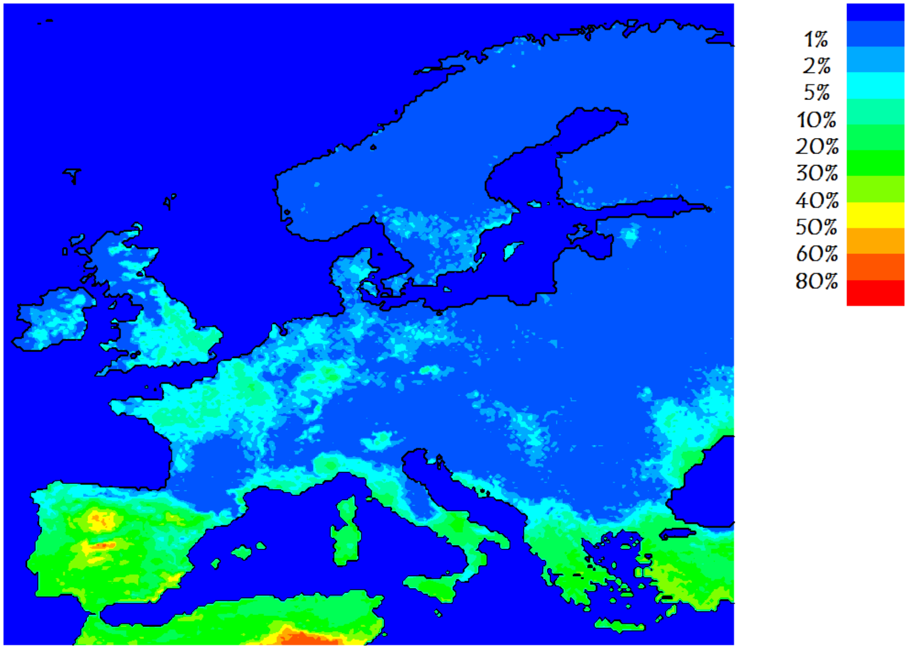

Fig. 6. Percentage of time with low flow "pool" conditions, derived from monthly duration curves for present climate.

HESSD
8, 4355–4379, 2011

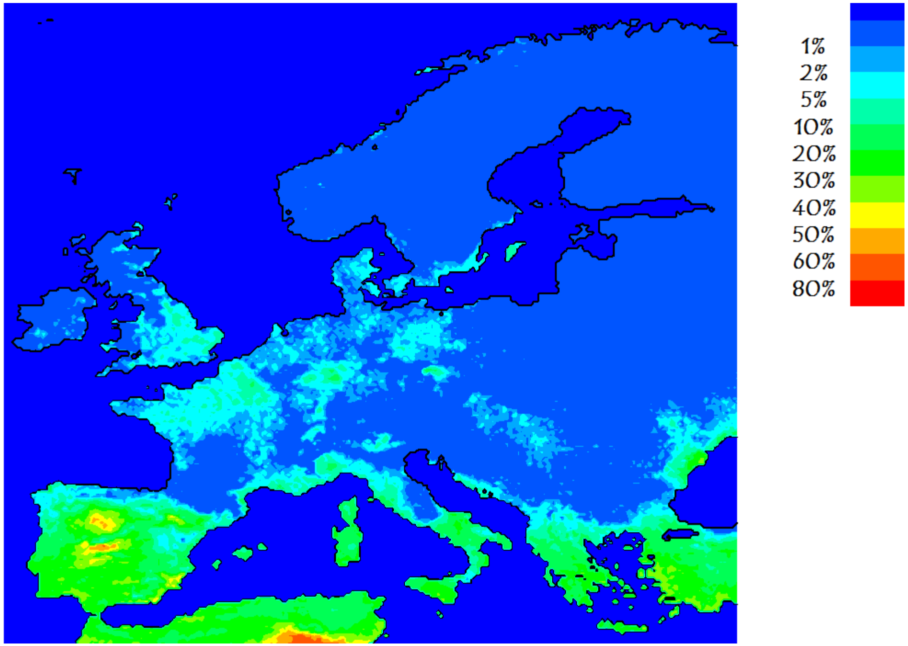

Fig. 7. Percentage of time with low flow "pool" conditions, derived from monthly duration curves with 2 °C warming.

HESSD

8, 4355–4379, 2011

Characterizing temporary hydrological regimes at a European scale

M. J. Kirkby et al.

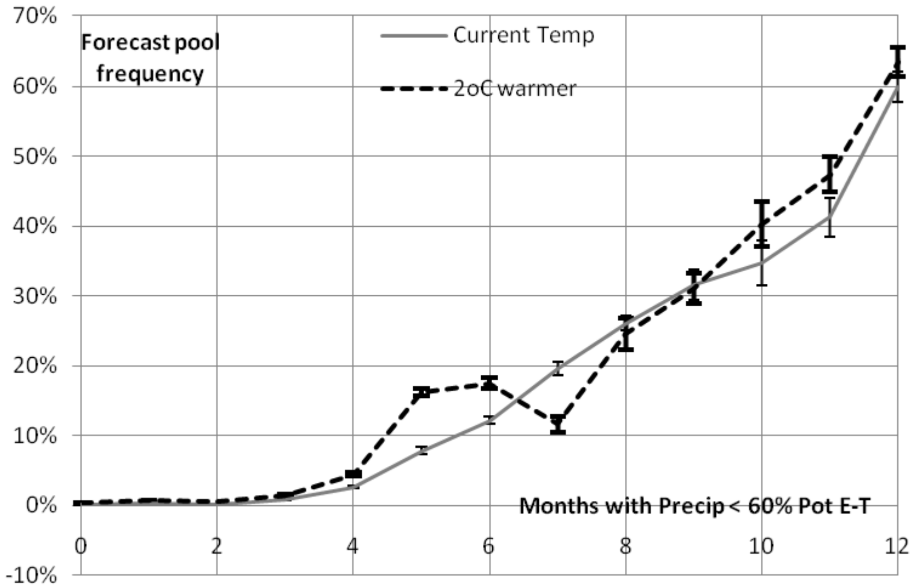

Fig. 8. Empirical relationship between forecast pool frequency and the average number of dry months (Precip < 0.6 Pot ET) for current climate and with a 2 °C temperature rise.